











## Research Article

# Clinical, Biochemical, and ATR-FTIR Spectroscopic Parameters Associated with Death or Survival in Patients with Severe COVID-19

**Adriana Martinez-Cuazitl** <sup>1,2</sup>, **Monica M. Mata-Miranda** <sup>1</sup>, **Miguel Sanchez-Brito** <sup>3</sup>,  
**Daniel Valencia-Trujillo** <sup>4</sup>, **Amanda M. Avila-Trejo** <sup>5</sup>, **Raul J. Delgado-Macuil** <sup>6</sup>,  
**Consuelo Atriano-Colorado** <sup>1</sup>, **Francisco Garibay-Gonzalez** <sup>1</sup>,  
**Virginia Sanchez-Monroy** <sup>7</sup> and **Gustavo J. Vazquez-Zapien** <sup>1,8</sup>

<sup>1</sup>Military School of Medicine, Military Center for Health Sciences, Ministry of National Defense, Mexico City 11200, Mexico

<sup>2</sup>National School of Medicine and Homeopathy, National Polytechnic Institute, Mexico City 07320, Mexico

<sup>3</sup>Superior School of Computing, National Polytechnic Institute, Mexico City 07738, Mexico

<sup>4</sup>Clinical Microbiology Service, National Institute of Respiratory Diseases, Mexico City 14080, Mexico

<sup>5</sup>National School of Biological Sciences, National Polytechnic Institute, Mexico City 07738, Mexico

<sup>6</sup>Applied Biotechnology Research Center, National Polytechnic Institute, Tlaxcala 90700, Mexico

<sup>7</sup>Superior School of Medicine, National Polytechnic Institute, Mexico City 11340, Mexico

<sup>8</sup>Research and Development Center of the Mexican Army and Air Force, Ministry of National Defense, Mexico City 11400, Mexico

Correspondence should be addressed to Gustavo J. Vazquez-Zapien; [gus1202@hotmail.com](mailto:gus1202@hotmail.com)

Received 6 October 2022; Revised 13 January 2023; Accepted 24 February 2023; Published 11 March 2023

Academic Editor: Feride Severcan

Copyright © 2023 Adriana Martinez-Cuazitl et al. This is an open access article distributed under the Creative Commons Attribution License, which permits unrestricted use, distribution, and reproduction in any medium, provided the original work is properly cited.

The wide range of symptoms of the coronavirus disease 2019 (COVID-19) makes it challenging to predict the disease evolution using a single parameter. Therefore, to describe the pathophysiological response to SARS-CoV-2 infection in hospitalized patients with severe COVID-19, we compared according to survival or death, the sociodemographic and clinical characteristics, the biochemical and immunological attenuated total reflection-Fourier transform infrared (ATR-FTIR) spectra from saliva samples and their correlation with chemometric findings. Herein, we demonstrate that ATR-FTIR spectroscopy allows the description of the events related to cell damage, such as lipids biogenesis and the secondary structure of proteins associated with lactate dehydrogenase and albumin levels. Moreover, humoral (IgM) and cellular (IFN- $\gamma$ , TNF- $\alpha$ , IL-10, and IL-6) responses were also increased in patients who died from COVID-19.

## 1. Introduction

Coronavirus disease 2019 (COVID-19), caused by severe acute respiratory syndrome coronavirus 2 (SARS-CoV-2), is still an urgent public health concern due to the consistent RNA modifications across the viral genome, provoking resistance to the vaccine, and infection-induced immunity. Moreover, acute infection is not the only outcome of COVID-19 but there is also the possibility of long-term COVID infection [1, 2].

The wide range of symptoms, complications, and outcomes generate many efforts to predict the evolution of the disease at an early stage, allow more time management and resource allocation, increase the cure rate, and decrease the case fatality rate [3–5].

Current knowledge of COVID-19 pathogenesis includes the direct cytopathic effects, ischemic injury, and host characteristics such as age, comorbidities, and aberrant immune responses; this might explain different disease presentations and severity [2, 6].

SARS-CoV-2 infects the host cells through the angiotensin-converting enzyme 2 (ACE2) receptor, which is on the X chromosome. It is expressed in cells and vessels of several organs, including the lung, heart, kidney, and intestine [6]. The spike protein (S) has a receptor-binding domain (RBD) in the S1 protein; this RBD interacts with the metallopeptidase domain of ACE2, triggering the endocytosis of the SARS-CoV-2 virion and exposing it to endosomal proteases. The S2 protein leads to membrane fusion and releases the viral package into the host cytoplasm [7]. CoVs display an envelope formed by a lipid bilayer derived from the host cell membranes due to the intracellular membrane, playing a pivotal role in coronavirus replications [6].

Coronaviruses can produce their proteins by attaching to the host ribosomes and generating single-stranded, negative-sense RNA (ssRNA<sup>-</sup>) that is used by the RNA polymerase to make ssRNA<sup>+</sup>, with the Golgi apparatus ssRNA<sup>+</sup>, which is packaged in the nucleocapsids to create new virion particles, which are then released by exocytosis. In this sense, infection, replication, and cell damage induce an immune response [8].

SARS-CoV-2 is recognized by several receptors such as Toll-like receptors (TLR) 3, 7, 8, and 9, RIG-I, and MDA5, which induce the type I interferon (IFN) response, provoking the formation of reactive oxidative species, calcium flux from cytoplasmic storages, protein aggregation, and the release of danger-associated patterns; at the same time, this contributes to the activation of the NLRP3 inflammasome. NLRP3 inflammasome induces caspase-1-dependent cleavage and release of key proinflammatory cytokines interleukin-1 $\beta$  (IL-1 $\beta$ ) and IL-18 and triggers gasdermin D-mediated pyroptotic cell death. As a result of pyroptotic cell death, the enzyme lactate dehydrogenase (LDH) is released, and levels of this enzyme correlate with disease severity. Also, SARS-CoV-2 can inhibit the type I IFN responses in infected cells, leading to an imbalanced immune response [2].

Besides, SARS-CoV-2 infection and the destruction of lung cells release cytokines and prime adaptive T and B cell immune responses. A wave of proinflammatory cytokines and chemokines is related to the increase of IL-6, IFN- $\gamma$ , MCP1, and IP-10, which are indicators of T helper 1 (TH1) cell polarized response [7]. These responses increase vascular permeability and adhesion molecule expression and recruit more immune cells, including neutrophils and monocytes. IL-8 recruits neutrophils, causing fluid leakage into the interstitial space and alveoli, resulting in interstitial and pulmonary edema. This can lead to dyspnea, impaired oxygenation, or hypoxemia. Hypoxemia stimulates chemoreceptors in the cardiopulmonary center of the brain, resulting in the development of tachypnea and tachycardia [8].

White blood cells (WBCs) and damaged endothelial cells release other inflammatory mediators, including arachidonic acid metabolites, leukotrienes, and prostaglandins, which provoke fever.

Also, IL-6 stimulates hepatocytes that produce acute-phase reactants such as C-reactive protein (CRP), fibrinogen, and hepcidin [8].

Moreover, specific humoral immunity against this virus plays an essential role in viral clearance; cytotoxic lymphocytes can eliminate infected cells, and specific antibody responses have the potential to neutralize the SARS-CoV-2 or help cytotoxic T cells, eliminating the virus from the infected cells to control disease progression. SARS-CoV-2 antigens induce B cells from germinal centers to proliferate and differentiate into plasma cells, triggering and releasing specific antibodies [9].

COVID-19 patients produce one or more specific antibodies against SARS-CoV-2; the main relevance of this response is related to serological diagnosis and prognosis prediction, such as levels of serum SARS-CoV-2-specific IgM, IgG, and IgA. Zheng et al. showed that elevated anti-SARS-CoV-2 IgG titers correlate with the length of hospitalization and are also associated with disease severity in a time-dependent manner, as demonstrated by the delayed IgG response observed in deceased patients [9, 10].

The antibody level reflects the dependence on the amide and lipid metabolisms; symptomatic patients have decreased levels of sphingosine consistent with the presence of acid ceramidase protein compared to asymptomatic patients [11].

In recent years, Fourier transform infrared (FTIR) spectroscopy has been used to differentiate between sick and healthy people by employing tissues, cells, and body fluids, as well as in the stratification of different diseases. In this sense, FTIR spectroscopy is a promising point-of-care technology for the classification of COVID-19 severity or measurement of periodic changes in COVID-19 antibody levels on serum or saliva samples [11–14].

With all this information, nowadays, there are many markers of prognosis and severity such as sex, age, comorbidities, WBC count, lymphocyte count, creatinine and bilirubin levels, as well as D-dimer, and C-reactive protein (PCR), lactate dehydrogenase (LDH), and viral load. Furthermore, many of these biomarkers change during the hospitalization stay, predicting the progression to severe disease [4, 10, 15].

Once FTIR spectroscopy changes could be related to these biomarkers, this technique seems helpful at any time point of patient hospital admission because it shows the biochemical and immunological status.

Therefore, our work compared the pathophysiological response to SARS-CoV-2 infection in hospitalized patients with a severe disease, divided into two groups according to their clinical evolution (survival and death groups). For this purpose, we analyzed the sociodemographic and clinical characteristics, the biochemical and immunological ATR-FTIR spectra from saliva samples, and their correlation with chemometric findings.

## 2. Materials and Methods

**2.1. Study Population.** The study was conducted at the Central Military Hospital (HCM)-SEDENA, Mexico. The study period was from May 19, 2020, to March 1, 2021.

In this research, we divided the population into survival and death groups. The survival group was integrated with COVID-19 patients who were hospitalized and those who

recovered from the illness, and the death group was composed of patients who died during the hospitalization.

The inclusion criteria were volunteers that accepted to participate in the study by writing informed consent, were aged over 18 years, diagnosed positive for COVID-19 by qRT-PCR test, category 3 risk factors for severe disease according to COVID-19 Treatment Guidance of Massachusetts General Hospital, and a fasting period of 8 hours. Contrarily, intubated patients and samples from patients who brushed or rinsed the oral cavity with mouthwash before sampling were excluded.

## 2.2. Medical Data Collection, Laboratories, and Evolution.

When the sample was collected, patients with symptoms (cough, dyspnea, headache, sputum, and fever, among others) and comorbidities such as diabetes, obesity, hypertension, and asthma were interrogated, and the obtained data were recorded as present or absent. To determine overweight and obesity, we followed the World Health Organization guidelines, which establish a body mass index (BMI)  $\geq 25$  for overweight and a BMI  $\geq 30$  for obesity [16].

At the same time, a blood sample for laboratory blood tests (hematic biometry, blood chemistry test, hepatic function test, and inflammatory biomarkers) was collected.

For the hematic biometry analysis, 5 ml of complete blood was collected in EDTA (ethylenediaminetetraacetic acid) tubes. Immediately, the blood sample was gently mixed and subjected to continued agitation for 30 minutes. After that, analysis was developed using ADVIA<sup>®</sup> 360 (SIEMS) equipment.

Five millilitres of blood were collected in a serum-separating tube for the blood chemistry test. After that, the blood sample was centrifuged at 1096g for ten minutes, and the obtained serum was collected and analyzed using the automatic equipment VITROS<sup>®</sup> 5600 (Ortho Clinical Diagnosis).

To evaluate clinical evolution, days of hospital stay were used as a time scale to calculate the median time for recovery or death.

**2.3. Saliva Sample Collection.** Both study groups were asked to donate 1 ml of saliva, collected in a sterile 1.5 ml microcentrifuge tube. The samples were kept cold (4°C) during their transfer and until their analysis in the following three hours. Personal protective equipment was used by personnel in charge of sampling and analyzing the samples. All experiments were evaluated and approved by the appropriate Ethics Committee, and the ethical standards laid down in the 1964 Declaration of Helsinki were followed. Moreover, the Institutional Human Research Ethical Committee approved the protocol and the written informed consent forms.

## 2.4. Saliva Sample Analysis through ATR-FTIR Spectroscopy.

The FTIR spectra analyzed in the attenuated total reflectance mode (ATR-FTIR spectra) were examined in the spectral range between 4000 and 400  $\text{cm}^{-1}$ , employing an

FTIR spectrometer (6600, Jasco). The apparatus has a fixed spectral resolution of 4  $\text{cm}^{-1}$ . For the sample analysis, three  $\mu\text{l}$  from the saliva were placed onto the ATR diamond crystal (PKS-D1F, Jasco). Subsequently, the sample was dried at room temperature for about 15 minutes to eliminate excess water until the band attributed to water was not detected [17]. The sample spectra were captured 120 times and averaged to obtain one spectrum. Each sample was analyzed in triplicate; then, the average of the spectra was obtained for the corresponding normalization and analysis.

**2.5. ATR-FTIR Spectrum Analysis.** Standard normal variate (SNV) normalization was performed employing the Unscrambler X software (version 10.3, Camo). Then, the second derivative spectra were determined by the Savitzky–Golay algorithm with five-point windows for smoothing and the second polynomial order using the Unscrambler X software. Next, the obtained spectra were inverted by factoring by  $-1$  [18]. Then, the mean of each population was obtained to identify relevant differences (displacements or area). The Origin software (version 8.5, Origin Lab Corporation) was used for getting the graphs.

ATR-FTIR analysis of lipids changes, such as the proportion of unbranched and branched molecules of lipids and fatty acids that could be related to cell damage, as well as the ratio of CH<sub>2</sub>/CH<sub>3</sub> area (2923 (2944–2915  $\text{cm}^{-1}$ )/2957 (2969–2952  $\text{cm}^{-1}$ )), the ratio of total area of lipids (2697–2952, 2944–2915, 2862–2845, 1753–1735, and 1475–1425)/total area of proteins (1674–1589, 1580–1504, and 1330–1301) [19], and the peak absorbance at 1075  $\text{cm}^{-1}$  were analyzed. In addition, using the second derivative, the areas related to urea (1475–1429  $\text{cm}^{-1}$ ) and the alpha helix/ $\beta$ -sheets ratio (1650 (1655–1649  $\text{cm}^{-1}$ )/A1626 (1627–1622  $\text{cm}^{-1}$ )) were calculated, which are related to SARS-CoV-2's induction of protein aggregates through its spike protein [14].

Moreover, humoral responses IgG, IgA, and IgM were evaluated by measuring the areas 1560–1464  $\text{cm}^{-1}$ , 1285–1237  $\text{cm}^{-1}$ , and 1160–1028  $\text{cm}^{-1}$ , respectively. In the same way, the cellular immune response was also analyzed through IL-6 (1428–1426  $\text{cm}^{-1}$ ), IL-1 $\beta$  (1409–1399  $\text{cm}^{-1}$ ), TNF- $\alpha$  (1243–1217  $\text{cm}^{-1}$ ), IFN- $\gamma$  (1061–1044  $\text{cm}^{-1}$ ), and IL-10 (1004–976  $\text{cm}^{-1}$ ) [13, 20].

**2.6. Statistical Analysis.** Descriptive nonparametric survival analysis, such as the Kaplan–Meier survival curve, was used to estimate survival probability. Days of hospital stays were used as a time scale to calculate the median time to recovery. Categorical variables were expressed as rate and percentage; for quantitative variables, normality tests were applied, and these were expressed as median  $\pm$  standard deviation (SD) media or interquartile range (IQR).  $\chi^2$ , Mann–Whitney U test, or T-student test, was used to determine significant differences between groups according to the variable type and normality of behavior. The analysis was performed using IBM SPSS Statistics 25.0 and Graph Pad 8.0.

### 3. Results

**3.1. Description of Patients.** From May 19, 2020, to March 1, 2021, 103 COVID-19 patients with category 3 risk factors for severe disease, according to the COVID-19 Treatment Guidance of Massachusetts General Hospital, and admitted to Central Military Hospital were recruited.

The median age was  $55 \pm 12.5$  years, and most patients were male. However, it is important to mention that patients who died (16.5%) were older ( $63 \pm 12$  years), highlighting that the majority of patients that integrated into this population were over 50 years old; nevertheless, no statistical significance was evidenced related to sex (Table 1).

**3.2. Baseline Clinical Characteristics of Patients.** The main comorbidities were being overweight, followed by diabetes and obesity, and had an O+ blood type. Patients who died showed major smoking; however, no statistical significance was observed between the groups. Regarding the blood type, the most common blood type in both groups was O+, followed by A+, without evidencing statistical significance. The main symptoms were dyspnea and cough; death patients showed more sputum compared with recovery patients. The ratio of arterial oxygen partial pressure to fractional inspired oxygen ( $\text{PaO}_2/\text{FiO}_2$ ) was low, and dead patients had a high respiratory rate (Table 2).

**3.3. Evolution of Patients.** Regarding the days at sampling and the hospital stay, no significant difference was evident; the Kaplan–Meier curve showed a median of 46.3 days. Nevertheless, it is essential to mention that 75% of dead patients required intubation and showed a median of 23.38 days (Table 3).

Figure 1(a) shows the mean ATR-FTIR spectra of both groups at  $4000\text{--}2800\text{ cm}^{-1}$  and the fingerprint region at  $1800\text{--}800\text{ cm}^{-1}$ . Figure 1(b) shows the biochemical components assigned to the peaks [14, 21–23], highlighting that most of the peaks showed a shift between the groups, except peaks 1, 7, and 9.

**3.4. Biochemical Characteristics of Patients by Serum and ATR-FTIR Analyses.** The death group showed higher creatinine, urea, CRP, and LDH, and lower lymphocyte and ALT levels than the survival group (Table 4).

Once lipid biogenesis pathways are related to the virus propagation, we analyzed this process through the 2923/2958 (CH<sub>2</sub>/CH<sub>3</sub>) ratio, the peak at  $1075\text{ cm}^{-1}$ , and the total area of lipids/total area of proteins ratio (Figure 2). Considering those above, the death group evidenced less lipid biogenesis (Figure 2(a)). Contrary, the peak at  $1075\text{ cm}^{-1}$ , related to phospholipids (Figure 2(b)), showed a higher content in the death group. Finally, regarding the total area of lipids/total area of proteins ratio, we did not find changes (Figure 2(c)).

The ATR-FTIR spectra analysis on the second derivative showed, in the death group, a decrease in the alpha helix of proteins and an increase in urea (Figures 3(a)–3(c)) according to the serum parameters.

**3.5. Immunology Changes in Serum and ATR-FTIR Analyses.** Figure 4(a) shows the mean of the triplicate in immunoglobulins regions, showing no significant differences in IgA and IgG. Contrarily, an increase in the IgM region was observed in dead patients (142.5 (105.3, 153.8)) in comparison with IgM in survival patients (125.1 (86.26, 147.9)), as shown in Figure 4(b). Moreover, the integrated area related to IgA was more significant in the death group (41.5 (36.06, 49.23)) than in the survival group (39.14 (28.12, 49.48)); contrarily, IgG was higher in the survival group (182.1 (132.1, 214.1)) than that in the death group (172 (146, 189.6)) (Figure 4(b)).

Patients who died showed higher levels of leucocytes, neutrophils, and N/L ratio; and low levels of lymphocytes (Table 5).

Finally, Figures 5(a) and 5(b) show the averaged and normalized spectra, raw and in the second derivative of the cytokine's regions, respectively, where there was an increase in IFN- $\gamma$ , IL-10, and IL-6 in the death group compared with the survival group, which was also seen in the integrated areas of the peaks, as shown in Figure 5(c).

### 4. Discussion

The COVID-19 pandemic remains unpredictable due to the spectrum of presentation varying from asymptomatic infection to a fulminant systemic inflammatory syndrome unleashed by the cytokine storm. Risk factors for mortality in COVID-19 reported in various studies include advanced age, male gender, and some comorbidities such as diabetes and hypertension [24].

On the other hand, Dessie and Zewotir showed a mortality rate between 3.14–61.51%, with a mortality prevalence among hospitalized patients of 17.62%, similar to our population (16.5%) [25].

Moreover, this research found significant aged patients in the death group; 88.2% of the deceased patients were >50 years old. Dessie and Zewotir declared that age is one of the main risk factors for death. Aging was associated with other viral infections such as MERS-CoV, SARS, and influenza, which might be related to lower immunity levels; it is known that aging reduces T cells' and B cells' clonal diversity and the dysregulated production of type 2 cytokines that could prolong the proinflammatory immune response, contributing to the poor outcomes [25, 26].

Furthermore, looking for a relationship between sex and death risk, we did not find any differences; however, the most predominant sex was male, similar to Alharbi et al., who also reported a majority of male hospitalized COVID-19 patients. Therefore, the women's advantages could be related to the immune regulatory genes on the X chromosome and the higher expression of TLR7 [5, 25].

Regarding the comorbidities, we found that the main comorbidities in both groups were overweight, but smoking was the most prevalent in the death group, which agrees with the meta-analysis of Brodin, who showed an association between COVID-19 progression and smoking. In addition, smoking depresses pulmonary immune function and is a risk factor for contracting other infectious diseases and

TABLE 1: Demographics of patients.

<i>N</i> (%)	COVID-19 <i>n</i> (%)	Survival <i>n</i> (%)	Dead <i>n</i> (%)	<i>p</i>
	103 (100)	86 (83.5)	17 (16.5)	
Age (years) media ± SD	55 ± 12.5	54 ± 12	63 ± 12	<b>0.006</b>
Age group	<i>n</i> (%)	Survival rate (%)	Dead rate (%)	<i>p</i> , $\chi^2$
>50 years	69/103 (67)	54/86 (62.8)	15/17 (88.2)	<b>0.041, 4.16</b>
Sex	Rate (%)	Sex rate (%)	Sex rate (%)	<i>p</i> , $\chi^2$
Men	75/103 (72.8)	60/75 (80)	15/75 (20)	
Women	28/103 (27.2)	26/28 (92.9)	2/28 (7.1)	0.118, 2.446

The bold values refer to statistical significance in each group.

TABLE 2: Comorbidities, blood type, symptoms, vital signs, and ponderal state.

	COVID-19 <i>n</i> (%)	Survival rate (%)	Dead rate (%)	<i>p</i> , $\chi^2$
<i>Comorbidities</i>				
Smoking	18 (17.5)	12/86 (14)	6/17 (35.3)	<b>0.045, 4.482</b>
Hypertension	31 (30.1)	24/86 (27.9)	7/17 (41.2)	0.209, 1.188
Overweight	47 (45.6)	41/86 (47.7)	6/17 (35.3)	
Obesity	32 (31.1)	29/86 (33.7)	3/17 (17.6)	<b>0.037, 6.589</b>
Diabetes	33 (32)	26/86 (30.2)	7/17 (41.2)	0.27, 0.781
Others (HIV, asthma, cancer, Parkinson, infertility)	6 (5.8)	3/86 (3.5)	3/17 (17.6)	0.055, 5.187
<i>Blood type</i>				
A+	16 (18.2)	10 (14.1)	6 (35.3)	
B+	2 (2.3)	2 (2.8)	0 (0)	
O-	2 (2.3)	2 (2.8)	0 (0)	0.188, 4.782
O+	68 (77.3)	57 (80.3)	11 (64.7)	
<i>Symptoms</i>				
Cough	72 (69.9)	60/86 (69.8)	12/17 (70.6)	0.597, 0.005
Fever	56 (54.4)	50/86 (58.1)	6/17 (35.3)	0.072, 2.986
Pharyngeal pain	33 (32)	26/86 (30.2)	7/17 (41.2)	0.27, 0.781
Dyspnea	75 (72.8)	64/86 (74.4)	11/17 (64.7)	0.293, 0.676
Headache	44 (42.7)	38/86 (44.2)	6/17 (35.3)	0.345, 0.459
Emesis	6 (5.8)	5/86 (5.8)	1/17 (5.9)	0.671, 0.0001
Sputum	38 (36.9)	28/86 (32.6)	10/17 (58.8)	<b>0.04, 4.206</b>
Arthralgias	41 (39.8)	36/86 (41.9)	5/17 (29.4)	0.249, 0.918
Myalgias	46 (44.7)	40/86 (46.5)	6/17 (35.3)	0.282, 0.723
<i>Vital signs and ponderal state</i>				
SaO <sub>2</sub> (%)	93 (91, 95)	93 (91, 95)	93 (89, 96)	0.523
PaO <sub>2</sub> /FiO <sub>2</sub>	242 (194, 332)	263 (190, 358)	219 (196, 233)	<b>0.002</b>
Heart rate (beats per minute)	80 ± 16	80 ± 16	79 ± 19	0.82
Respiratory rate (breaths per minute)	20 (19, 20)	19 (19, 20)	21 (20, 23)	<b>0.011</b>
Systolic (mmHg)	121 ± 21	120 ± 19	129 ± 30	0.127
Diastolic (mmHg)	73 ± 12	73 ± 12	73 ± 14	0.924
Mean arterial pressure (mmHg)	89 ± 15	88 ± 14	92 ± 18	0.424
BMI (kg/m <sup>2</sup> )	28.5 ± 4.5	28.8 ± 4.3	26.9 ± 5.5	0.126

The bold values refer to statistical significance in each group.

more severe outcomes among people who become infected; also, it is reported that cigarette smoke induces expression of ACE2, which allows SARS-CoV-2 to enter cells [2, 25, 27].

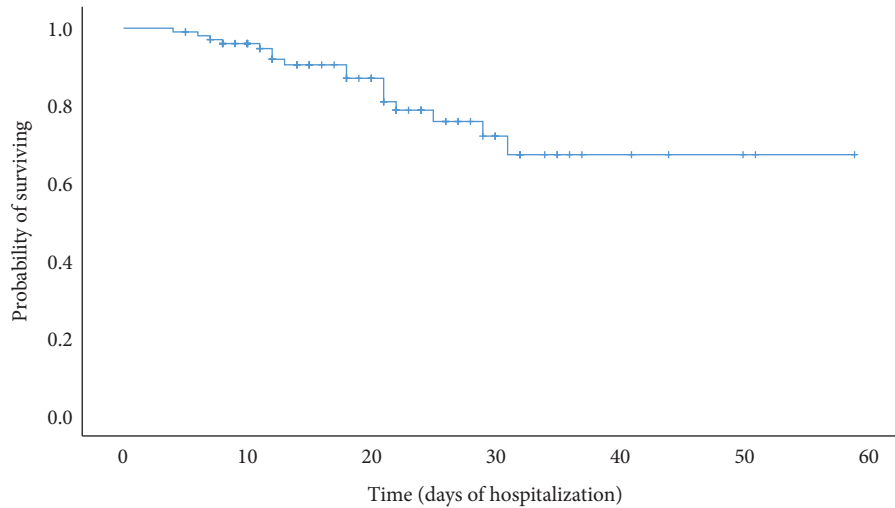
About the symptoms, it has been reported that the natural evolution of COVID-19 involved a 4–5 days incubation period, showing fever and dry cough at admission time, followed by dyspnea, arthralgias, myalgias, and headache. Herein we found that the main symptom on sampling day (8 days) was cough. It is essential to mention that eight days is when severe COVID-19 cases progress to acute respiratory distress syndrome (ARDS) [7]. ARDS may lead directly to respiratory failure, which is the cause of death in 70% of fatal COVID-19 cases and 52.9% of intubated patients death (9/17 patients).

Regarding the days of hospitalization, in our study, we found a median of 18 days of hospital stay, similar to that reported by Garibaldi et al., who showed a median of 19 days (IQR, 11.9 to 30.0 days). Regarding our Kaplan–Meier analysis, including all patients, it showed a median of 46.3 days, while it was 23.38 days in intubated patients. In contrast, the same study of Garibaldi showed that the median time for intubation was 66.5 days [15].

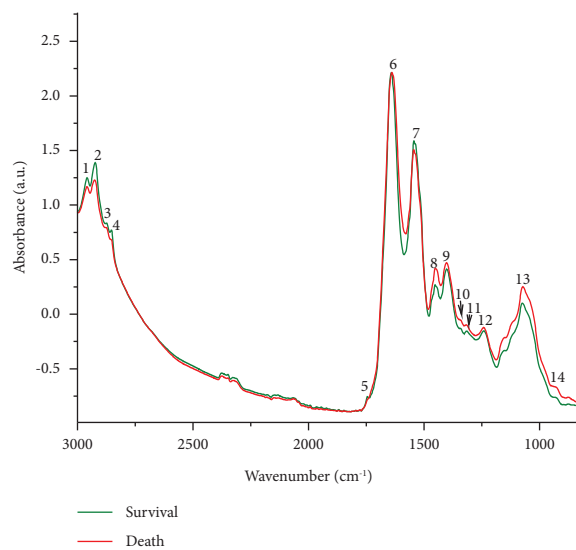
Concerning ATR-FTIR results, shifts in the spectra are reported on serum between COVID-19 patients and standard controls, indicating protein and lipid conformation changes according to biochemical and immunological changes described below [28].

TABLE 3: Evolution of patients.

Evolution	COVID-19 $n$ (%)	Survival $n$ (%)	Death $n$ (%)	$p$ , $\chi^2$
Sampling day	8 (5, 15)	8 (5, 15)	6 (3, 8)	0.059
Intubation rate (%)	12/103 (11.7)	3/86 (3.5)	9/17 (52.9)	<b>0.0001, 33.724</b>
Hospitalization stay (days)	18 (10, 26)	16 (10, 26)	18 (11, 21)	0.4



The bold values refer to statistical significance in each group.



(a)

FIGURE 1: Continued.

Peak	Assignment	Survival median	Death median	P
1	$V_{as}CH_3$ lipids, DNA and proteins	2958.268	2958.268	0.074
2	$V_{as}CH_2$ lipids, fatty acids	2923.556	2926.448	0.0001
3	$V_sCH_3$	2874.38	2877.273	0.0001
4	$V_sCH_2$ , lipids, fatty acids	2853.167	2858.952	0.0001
5	$\nu CO$ lipids, triglycerides, polysaccharides	1744.7805	1740.441	0.0001
6	Amide I (C=O <i>str</i> )	1641.125	1633.411	0.0001
7	Amide II ( $\nu CN$ <i>str</i> , NH bending)	1542.774	1544.702	0.103
8	$CH_2/CH_3$	1452.136	1451.171	0.0001
9	C=O <i>str</i> of -COO <sup>-</sup>	1401.995	1401.995	0.506
10	Carboxyl groups COO and asymmetric C-N stretching	1345.106	1347.998	0.036
11	Amino acid side-chains; terminal oxygen ( $PO_3^-$ )	1314.25	1316.179	0.0001
12	Amide III/phospholipids	1240.969	1241.933	0.003
13	Glycosylated proteins and phosphorus-containing components	1075.12	1072.228	0.0001
14	Nucleic acids	946.8773	942.0561	0.047

(b)

FIGURE 1: ATR-FTIR spectra of saliva samples of hospitalized patients with severe COVID-19 who survived or died. (a) Mean of the ATR-FTIR spectra of both groups, including the biological fingerprint region at  $1800-800\text{ cm}^{-1}$ . (b) Biochemical components assignment to the peaks.  $p$  represents the statistical significance after the Mann-Whitney U analysis.

TABLE 4: Biochemical parameters on hospitalized patients with severe COVID-19.

	COVID-19 Media (IQR)	Survival Media (IQR)	Death Media (IQR)	$p$
<i>Blood chemistry test</i>				
Creatinine (mg/dL)	0.7 (0.6, 0.8)	0.7 (0.5, 0.8)	0.8 (0.7, 1.2)	<b>0.005</b>
Urea (mg/dL)	38.5 (30, 50.3)	36.4 (27.8, 47.1)	66.3 (55.6, 96.3)	<b>0.0001</b>
Glucose (mg/dL)	121 (91.5, 165.5)	119 (87, 161)	154 (131, 178)	0.081
<i>Serum electrolytes</i>				
Na (mmol/L)	137 (135, 139)	137 (135, 139)	138 (136, 139)	0.943
K (mmol/L)	4.3 (3.9, 4.6)	4.2 (3.9, 4.6)	4.8 (4.3, 5.1)	0.093
<i>Hepatic-function test</i>				
ALT (U/L)	43 (29, 72)	49.5 (31, 75)	29 (20, 43)	<b>0.01</b>
AST (U/L)	34 (25, 43.5)	34 (25, 44)	30 (23, 41)	0.599
ALP (U/L)	87 (72, 122.5)	88 (69, 123)	85 (76, 121)	0.652
Albumin (g/dL)	3 (2.7, 3.3)	3.1 (2.8, 3.4)	2.7 (2.6, 3.0)	<b>0.004</b>
<i>Inflammatory markers</i>				
CRP (mg/dL)	22.6 (8.7, 126.5)	18.9 (7.0, 70.3)	131.3 (57.1, 169.0)	<b>0.0001</b>
LDH (UI/L)	269 (222.5, 350)	131 (57, 169)	380 (305, 602)	<b>0.0001</b>
Fibrinogen (mg/dL)	461 (364, 701.5)	444 (477, 476)	611 (477, 746)	0.099

The bold values refer to statistical significance in each group.

Moreover, shifts on bands at  $2923\text{ cm}^{-1}$ ,  $2853\text{ cm}^{-1}$ ,  $1240\text{ cm}^{-1}$ , and  $1075\text{ cm}^{-1}$  suggest the potential conformational changes in lipid components; lipid biogenesis pathways affect receptor-mediated virus entry at the endosomal cell surface and modulate virus propagation [29].

Lipid changes are corroborated by the decreased ratio of  $2923/2958$  ( $CH_2/CH_3$ ) in dead patients; this ratio shows the

proportion of unbranched and branched molecules of lipids and fatty acids that also are associated with cell damage like apoptosis [30].

In the same way, changes in the ratio related to  $CH_2/CH_3$  might reflect an increase in the intermolecular chain disorder; the higher concentration of a long chain of  $CH_2$  suggests a weakening of the cell membrane-skeleton

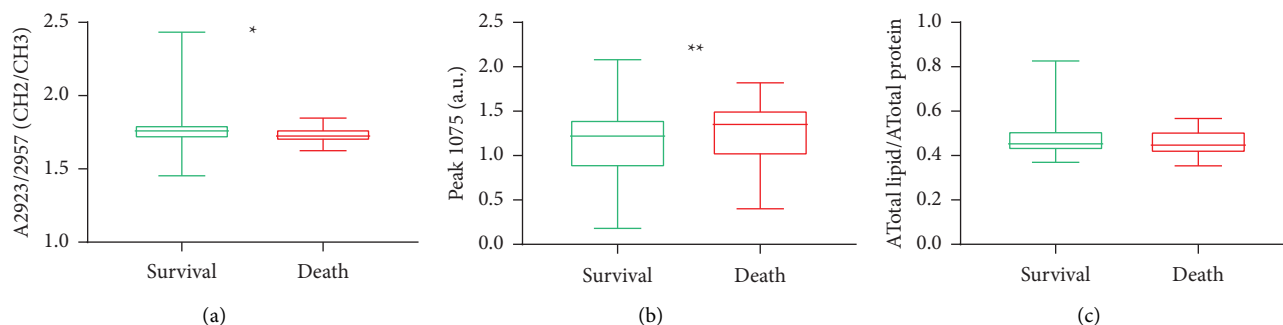


FIGURE 2: Lipids analysis using ATR-FTIR spectra (median and RIQ) on hospitalized patients with severe COVID-19 who survived or died. (a) CH2/CH3 ratio. (b) 1075 peak absorbance. (c) Total area of lipids/total area of proteins ratio. Mann-Whitney U analysis. \*  $p < 0.05$ , \*\*  $p < 0.005$ .

structure. That is according to the findings of Bel'skaya, who reported a significant decrease in polysaturated fatty acids with the main content of CH2, such as palmitic acid. The decrease in palmitic acid could be related to the requirement of lipid chains by the SARS-CoV-2; the process of cysteine palmitoylation regulates lipid addition to conserved cysteine residues that are located adjacent to the transmembrane sections of the virus spike and envelope proteins, which has also been demonstrated on influenza A virus; in addition, the decrease in the activity of the 19-desaturase [30–34].

Likewise, in comparison with healthy patients, an increase in oleic, linoleic, and arachidonic acids in COVID-19 patients has also been reported [30, 35]. Oleic acid modulates the inflammatory process, apoptosis, necrosis, and oxidative stress, and it stimulates iNOS and oleic acid increase by decreasing the activity of D9-desaturases on the phospholipids. Although the linoleic acid increase could be related to damage to mitochondrial dysfunction, modulated by the SARS-CoV-2 infection, higher levels of arachidonic acid are a part of a defense mechanism that can cause inflammation and modulate the development of the cytokine storm [32].

About phospholipids, the band at  $1075\text{ cm}^{-1}$  attributed to this component, specifically sphingomyelin and lysolecithin (symmetric stretches from  $\text{PO}_2^-$ ), increased in the death group; other studies have also shown that in the mild, severe, and fatal COVID-19 patients, they are higher [28].

Related to the protein changes, the amide I band shifts  $10\text{ cm}^{-1}$ , suggesting transitions in protein secondary structures. This has been reported by Zhang et al. In this research, we found that the proportion in the 1650/1626 area is related to changes in the conformational structure of proteins  $\alpha$ -helix/ $\beta$ -pleated sheet; this ratio decreased in the death group. In the same way, a decrease in  $\alpha$ -helix and an increase in  $\beta$ -pleated sheet structure were evidenced; those are related to a reduction in albumin that predominates the  $\alpha$ -helix structure, and an increase in immunoglobulins correlate with the increase of the  $\beta$ -pleated sheet [28].

Regarding the ratio of total lipids area/total proteins area, we did not find changes; in this way, the changes in the acyl chain length of lipids can serve as an indicator of more subtle differences in the structure of lipids that are not related to the total content of proteins [19].

The changes in lipids and proteins are related to the cytopathogenesis effect of the SARS-CoV-2 infection, which could be related to increased lactate dehydrogenase (LDH) levels in dead patients. In the same way, LDH could be related to the necrosis process. While CRP is an inflammatory marker, LDH is usually employed as a marker of cell damage, and it has been associated with the severity of COVID-19. LDH is an enzyme involved in carbohydrate metabolism by the conversion of lactate and pyruvate. Abnormal LDH levels can result from decreased oxygenation, leading to an upregulation of the glycolytic pathway and multiple organ injuries. In cell damage, LDH is released, and high levels also have an unfavorable prognosis in other pathologies, e.g., infections, malignancies, sepsis, or cardiopulmonary compromise [6, 24, 36–39].

Here, we found a significant decrease in serum levels of albumin and an increase in CRP in the dead group; the reduction in the albumin level is related to the acute phase response of patients to viral infection with an increase in CRP. The decrease in hepatic synthesis of proteins is associated with dysregulation of hepatic function; even though the significant ALT levels are in survival patients, we also find increased levels of ALT 43 U/L (29, 72 U/L) when compared with the previous report of 26.20 U/L (17.00–53.00 U/L), suggesting hepatic dysfunction [28, 40].

Biochemical changes are related to mortality, such as an increase in AST, ALT, urea, creatinine, and CRP, that are similar to our findings in serum levels and ATR-FTIR analysis, such as urea area peaks elevated at  $1452\text{ cm}^{-1}$  [1, 3, 24, 41].

In severe respiratory failure and death, multiple studies suggest that the dysregulated immune response is one of the main factors [10].

Lasso et al. showed that the higher peak of IgG correlates with the length of hospitalization and disease severity in a kinetic assay during the hospitalization stay, but they did not find any significant difference at admission. Likewise, herein, at the time of the sampling test, we did not find any change in IgG levels by ATR-FTIR spectroscopy; according to the findings of Lasso et al., they showed similar IgG responses in severe and mild patients [10, 42].

The increase in IgM area ( $1160\text{--}1028\text{ cm}^{-1}$ ) was significantly lower in the survival group than in the death group.



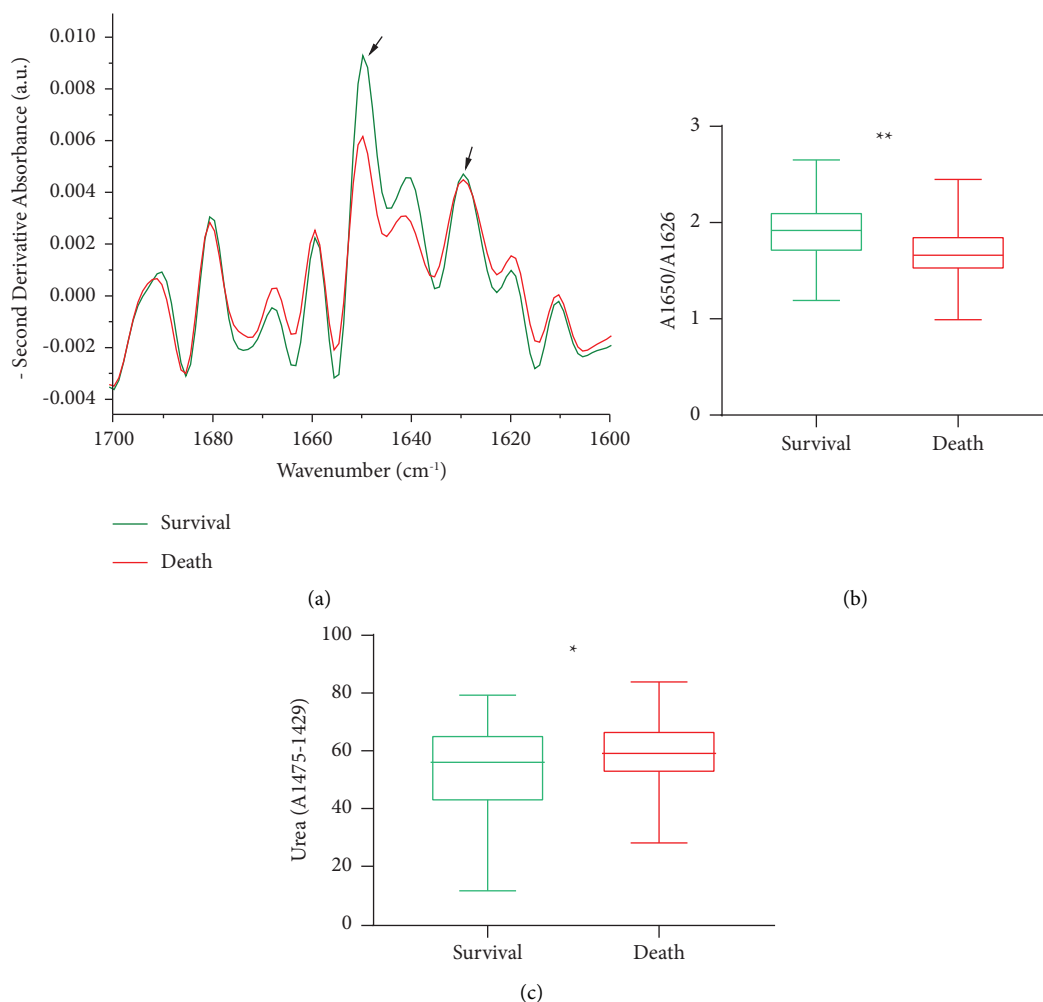


FIGURE 3: Proteins region analysis on hospitalized patients with severe COVID-19 who survived or died. (a) Second derivative of the ATR-FTIR spectra in the amide I region. (b) Alpha helix/ $\beta$ -sheets (median and RIQ) area ratio. (c) Urea peak (median and RIQ). U-Mann-Whitney analysis. \*  $p < 0.05$ , \*\*  $p < 0.005$ .

About this, Martinez-Cuazitl et al. demonstrated that IgM is lower in mildly COVID-19 patients in comparison with severely ill patients [13, 42]. One explanation is an antibody-dependent enhancement (ADE), a phenomenon described for infections with viruses such as dengue. ADE occurs when the antibody does not block the viral entry; the antibody might facilitate Fc-receptor-mediated endocytosis of the virus, enhanced viral replication, and massive inflammatory responses [2].

Lasso et al. and many other studies showed higher levels of leukocytes, neutrophils, and low levels of lymphocytes in dead patients, similar to our findings. The lymphopenia could be explained by apoptosis, according to the lipids and LDH changes described before [10, 24, 37, 43, 44].

Also, the lymphopenia and increased neutrophil-lymphocyte ratio seen in patients with SARS-CoV-2 infection may be explained due the secretion of such cytokines and chemokines (IL-6, IFN- $\gamma$ , MCP1, and IP-10), inducing the recruitment of immune cells from the blood and the infiltration of lymphocytes into the airways [7].

Severe symptoms of COVID-19 and death patients showed an increased serum concentration of many proinflammatory mediators such as IL-10, IL-6, IL-1 $\beta$ , TNF- $\alpha$ , and IFN- $\gamma$ , which is correlated with lymphopenia, and infiltration of hyperactive mononuclear cells in the lungs, that is according to our findings. Furthermore, although we did not find significant differences in IL-6 and IL-1 $\beta$ , high levels of these interleukins in the death group were evident [45].

The immune response against severe SARS-CoV-2 infection is characterized by a combination of delayed-type I/III interferon response and production of proinflammatory cytokines that recruit effector cells; type III IFNs are structurally related to IL-10 family cytokines, that is, according to our findings by ATR-FTIR that increase IL-10 on death patients [10, 46].

In addition, the increase of type II interferon (IFN- $\gamma$ ) is secreted by natural killer and T cells but not directly by virus-infected cells; IFN- $\gamma$  activates macrophages that induce more proinflammatory cytokines, dysregulating the immune system. Also, higher levels of IFN- $\gamma$  are related to the CRP levels described by Paolini et al. [44, 47].

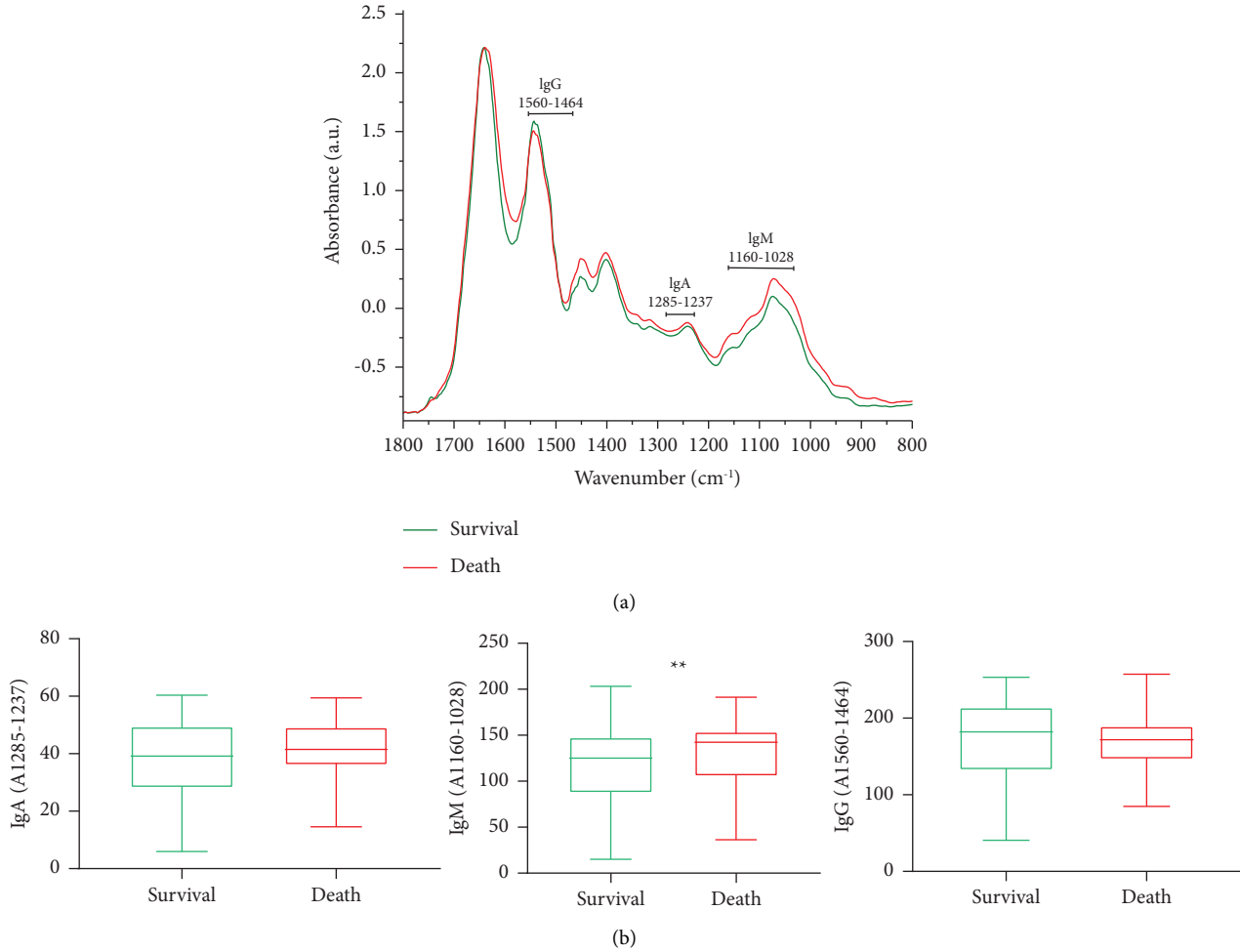


FIGURE 4: Immunoglobulins content on hospitalized patients with severe COVID-19 who survived or died. (a) ATR-FTIR spectra of the immunoglobulin's regions in the fingerprint region. (b) IgA, IgM, and IgG (median and RIQ) levels. Mann-Whitney U test. \*\*  $p < 0.005$ .

TABLE 5: Inflammatory response, hemoglobin, and platelets levels in hospitalized patients with severe COVID-19.

	COVID-19 Media (IQR)	Survival Media (IQR)	Death Media (IQR)	$p$
<i>Hematic biometry</i>				
Leukocytes ( $10^3/\mu\text{l}$ )	7.78 (5.9, 10.5)	7.38 (5.8, 9.3)	12.1 (8.6, 14.1)	<b>0.001</b>
Neutrophils ( $10^3/\mu\text{l}$ )	5.9 (4.3, 8.1)	5.6 (4, 7.7)	10.9 (7.9, 12.8)	<b>0.0001</b>
Lymphocytes ( $10^3/\mu\text{l}$ )	0.85 (0.6, 1.2)	0.89 (0.63, 1.31)	0.61 (0.41, 0.77)	<b>0.0001</b>
N/L ratio	7.2 (4, 12)	7 (4, 9)	18 (9, 24)	<b>0.0001</b>
Hemoglobin (g/dl)	14.6 (13.3, 15.4)	14.6 (13.4, 15.3)	14.5 (12.5, 15.9)	0.628
Platelets ( $10^3/\mu\text{l}$ )	295 (229, 374)	288 (217, 371)	325 (246, 383)	0.689

The bold values refer to statistical significance in each group.

In another way, the cell death pathways (apoptosis, necroptosis, and proptosis) induced by SARS-CoV-2 infection could be modulated by the higher levels of tumor necrosis factor (TNF) and IFN- $\gamma$ . The cell death is directly correlated with lung injury, multiple organ failure, and critical prognosis [44].

The increase in cell death also could be regulated by the NLR family pyrin domain containing 3 (NLRP3) inflammasome that induces pyroptotic cell death mediated by the caspase-1 dependent cleavage and release the IL1- $\beta$ , increasing LDH levels, as our findings [2].

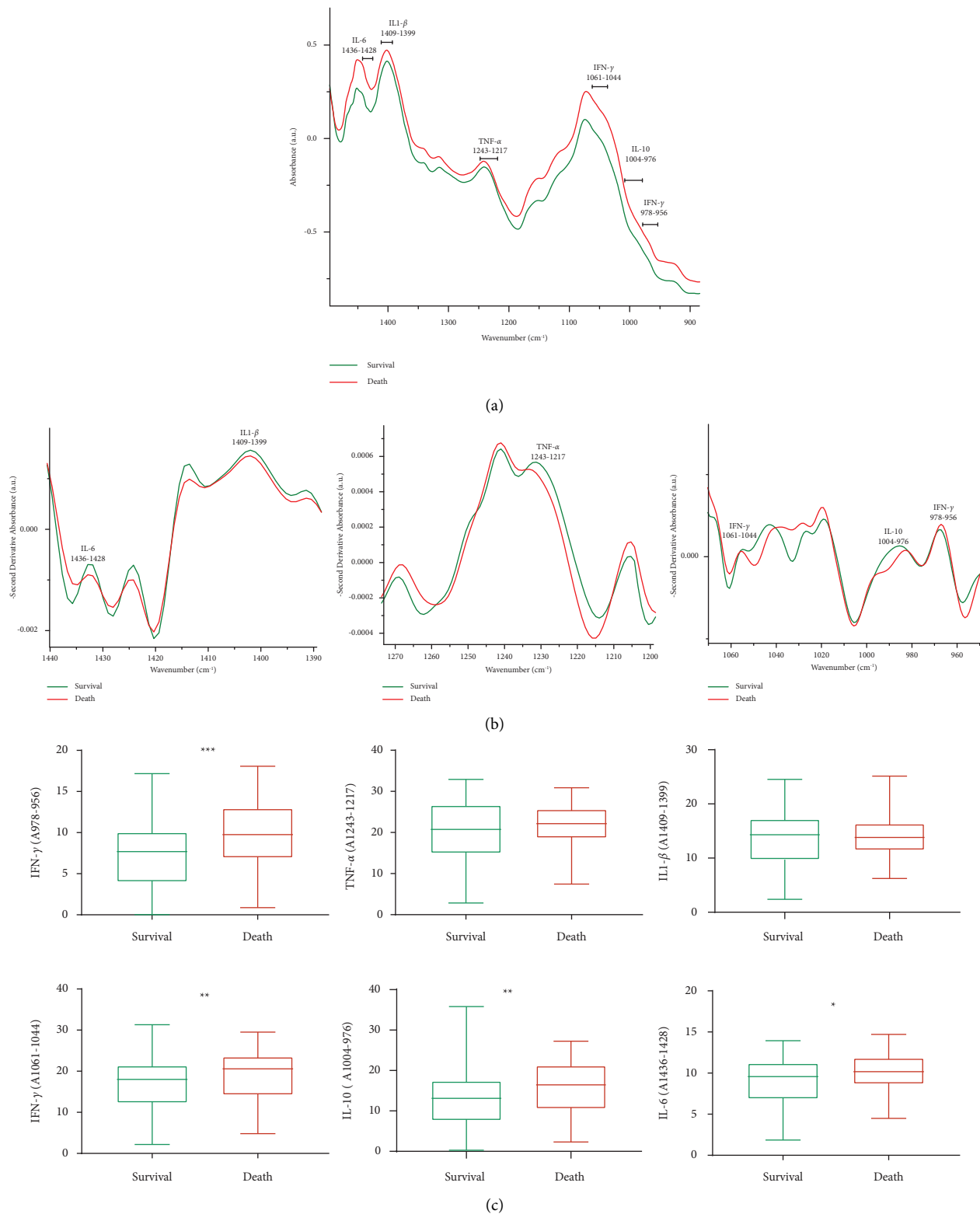


FIGURE 5: Cytokines content on hospitalized patients with severe COVID-19 who survived or died. (a) ATR-FTIR spectra of the cytokine's regions. (b) Second derivative of the ATR-FTIR spectra of the analyzed cytokines. (c) IFN- $\gamma$ , TNF- $\alpha$ , IL1- $\beta$ , IL-10, and IL-6 (median and RIQ) levels. U-Mann-Whitney analysis. \*  $p < 0.05$ , \*\*  $p < 0.005$ , \*\*\*  $p < 0.0005$ .

## 5. Conclusions

Here, we showed that patients in the death group were older, overweight, and smokers. Moreover, it is essential to mention that it showed a higher respiratory rate than the survival group.

ATR-FTIR spectroscopy allowed to establish an association between clinical course (survival or death) and biochemical and immunological status once a decrease in lipid biogenesis pathways was evidenced as well as an increment of phospholipids, which are related to virus propagation and cell damage in the death group.

Shifts in the amide I band, a decrease in the  $\alpha$ -helix/ $\beta$ -pleated sheet related to the reduction of albumin and increase of urea, and immunoglobulin production, especially IgM, demonstrate the host cell damage induced by the SARS-CoV-2 infection.

Cell damage also induces the cellular immune response that modulates the cytokines IL-10, IL-6, IL-1 $\beta$ , TNF- $\alpha$ , IFN- $\gamma$ , and the lymphopenia shown in the death group, also reflected in higher levels of inflammatory markers (CRP and LDH).

## Data Availability

All the generated data and the analysis developed in this study are included within the article.

## Ethical Approval

The Clinical Research Ethics Committee of the Hospital Central Militar of the Secretaria de la Defensa Nacional approved the protocol and informed consent.

## Conflicts of Interest

The authors declare that they have no conflicts of interest.

## Authors' Contributions

A.M.C., M.M.M.M., and G.J.V.Z. designed the project, planned the experiments, and wrote the manuscript. M.S.B., D.V.T., A.M.A.T., and C.A.C. performed the experiments. R.J.D.M., F.G.G., and V.S.M. provided important suggestions about manuscript writing. All authors reviewed the manuscript.

## Acknowledgments

The authors thank Melissa Guerrero-Ruiz, Jesús Benjamin Solano-Sanchez, Arleth S. Chavez-Velasco, Charlyn Valadez-Zenteno, and the people who kindly agreed to participate in the project and provided a saliva sample. This work was supported by the A022-2021 (SEDENA) budgetary program from the C.I.D.E.F.A.M.

## References

[1] G. Tiecco, S. Storti, S. Arsuffi et al., "2 lineage, the "stealth" variant: is it truly a silent epidemic? A literature review,"

- International Journal of Molecular Sciences*, vol. 23, no. 13, p. 7315, 2022.
- [2] P. Brodin, "Immune determinants of COVID-19 disease presentation and severity," *Nature Medicine*, vol. 27, no. 1, pp. 28–33, 2021.
- [3] H. H. Assal, H. M. Abdel-hamid, S. Magdy et al., "Predictors of severity and mortality in COVID-19 patients," *Egypt J Bronchol*, vol. 16, no. 1, p. 18, 2022.
- [4] R. S. Loomba, E. G. Villarreal, J. S. Farias, G. Aggarwal, S. Aggarwal, and S. Flores, "Serum biomarkers for prediction of mortality in patients with COVID-19," *Annals of Clinical Biochemistry*, vol. 59, no. 1, pp. 15–22, 2022.
- [5] A. A. Alharbi, K. I. Alqumaizi, I. Bin Hussain et al., "Characteristics of hospitalized COVID-19 patients in the four southern regions under the proposed southern business unit of Saudi Arabia," *International Journal of General Medicine*, vol. 15, pp. 3573–3582, 2022.
- [6] R. Nardacci, F. Colavita, C. Castilletti et al., "Evidences for lipid involvement in SARS-CoV-2 cytopathogenesis," *Cell Death & Disease*, vol. 12, no. 3, p. 263, 2021.
- [7] M. Z. Tay, C. M. Poh, L. Rénia, P. A. MacAry, and L. F. P. Ng, "The trinity of COVID-19: immunity, inflammation and intervention," *Nature Reviews Immunology*, vol. 20, no. 6, pp. 363–374, 2020.
- [8] S. Rahman, M. T. V. Montero, K. Rowe, R. Kirton, and F. Kunik Jr, "Epidemiology, pathogenesis, clinical presentations, diagnosis and treatment of COVID-19: a review of current evidence," *Expert Review of Clinical Pharmacology*, vol. 14, no. 5, pp. 601–621, 2021.
- [9] J. Zheng, Y. Deng, Z. Zhao et al., "Characterization of SARS-CoV-2-specific humoral immunity and its potential applications and therapeutic prospects," *Cellular and Molecular Immunology*, vol. 19, no. 2, pp. 150–157, 2022.
- [10] G. Lasso, S. Khan, S. A. Allen et al., "Longitudinally monitored immune biomarkers predict the timing of COVID-19 outcomes," *PLoS Computational Biology*, vol. 18, no. 1, Article ID e1009778, 2022.
- [11] Z. Guleken, Y. Tuyji Tok, P. Jakubczyk et al., "Development of novel spectroscopic and machine learning methods for the measurement of periodic changes in COVID-19 antibody level," *Measurement*, vol. 196, Article ID 111258, 2022.
- [12] A. Banerjee, A. Gokhale, R. Bankar et al., "Rapid classification of COVID-19 severity by ATR-FTIR spectroscopy of plasma samples," *Analytical Chemistry*, vol. 93, no. 30, pp. 10391–10396, 2021.
- [13] A. Martinez-Cuazitl, G. J. Vazquez-Zapien, M. Sanchez-Brito et al., "ATR-FTIR spectrum analysis of saliva samples from COVID-19 positive patients," *Scientific Reports*, vol. 11, no. 1, Article ID 19980, 2021.
- [14] S. T. Kazmer, G. Hartel, H. Robinson et al., "Pathophysiological response to SARS-CoV-2 infection detected by infrared spectroscopy enables rapid and robust saliva screening for COVID-19," *Biomedicine*, vol. 10, no. 2, p. 351, 2022.
- [15] B. T. Garibaldi, J. Fiksel, J. Muschelli et al., "Patient trajectories among persons hospitalized for COVID-19 a cohort study," *Annals of Internal Medicine*, vol. 174, no. 1, pp. 33–41, 2021.
- [16] World health organization, "Obesity and overweight," 2021, <https://www.who.int/news-room/fact-sheets/detail/obesity-and-overweight>.
- [17] R. Brogna, H. Oldenhof, H. Sieme, and W. F. Wolkers, "Spectral fingerprinting to evaluate effects of storage conditions on biomolecular structure of filter-dried saliva samples

- and recovered DNA,” *Scientific Reports*, vol. 10, no. 1, Article ID 21442, 2020.
- [18] H. Yang, S. Yang, J. Kong, A. Dong, and S. Yu, “Obtaining information about protein secondary structures in aqueous solution using Fourier transform IR spectroscopy,” *Nature Protocols*, vol. 10, no. 3, pp. 382–396, 2015.
- [19] A. Dogan, R. Gurbanov, M. Severcan, and F. Severcan, “CoronaVac (Sinovac) COVID-19 vaccine-induced molecular changes in healthy human serum by infrared spectroscopy coupled with chemometrics,” *Turkish Journal of Biology*, vol. 45, no. 1, pp. 549–558, 2021.
- [20] G. J. Vazquez-Zapien, A. Martinez-Cuazitl, M. Sanchez-Brito et al., “Comparison of the immune response in vaccinated people positive and negative to SARS-CoV-2 employing FTIR spectroscopy,” *Cells*, vol. 11, no. 23, p. 3884, 2022.
- [21] L. V. Bel’skaya, E. A. Sarf, and N. A. Makarova, “Use of fourier transform IR spectroscopy for the study of saliva composition,” *Journal of Applied Spectroscopy (Translation of Zhurnal Prikladnoi Spektroskopii)*, vol. 85, no. 3, pp. 445–451, 2018.
- [22] D. R. Paschotto, B. Pupin, T. T. Bhattacharjee, and L. E. S. Soares, “Saliva preparation method exploration for ATR-FTIR spectroscopy: towards bio-fluid based disease diagnosis,” *Analytical Sciences*, vol. 36, no. 9, pp. 1059–1064, 2020.
- [23] I. C. C. Ferreira, E. M. G. Aguiar, A. T. F. Silva et al., “Attenuated total reflection-fourier transform infrared (ATR-FTIR) spectroscopy analysis of saliva for breast cancer diagnosis,” *Journal of Oncology*, vol. 2020, Article ID 4343590, 11 pages, 2020.
- [24] N. Gopalan, S. Senthil, N. L. Prabakar et al., “Predictors of mortality among hospitalized COVID-19 patients and risk score formulation for prioritizing tertiary care-An experience from South India,” *PLoS One*, vol. 17, no. 2, Article ID e0263471, 2022.
- [25] Z. G. Dessie and T. Zewotir, “Mortality-related risk factors of COVID-19: a systematic review and meta-analysis of 42 studies and 423,117 patients,” *BMC Infectious Diseases*, vol. 21, no. 1, p. 855, 2021.
- [26] S. Molani, P. V. Hernandez, R. T. Roper et al., “Risk factors for severe COVID-19 differ by age for hospitalized adults,” *Scientific Reports*, vol. 12, no. 1, p. 6568, 2022.
- [27] R. Patanavanich and S. A. Glantz, “Smoking is associated with COVID-19 progression: a meta-analysis,” *Nicotine & Tobacco Research*, vol. 22, no. 9, pp. 1653–1656, 2020.
- [28] L. Zhang, M. Xiao, Y. Wang et al., “Fast screening and primary diagnosis of COVID-19 by ATR-FT-IR,” *Analytical Chemistry*, vol. 93, no. 4, pp. 2191–2199, 2021.
- [29] M. Caterino, M. Gelzo, S. Sol et al., “Dysregulation of lipid metabolism and pathological inflammation in patients with COVID-19,” *Scientific Reports*, vol. 11, no. 1, p. 2941, 2021.
- [30] L. V. Bel’skaya, E. A. Sarf, and V. K. Kosenok, “Analysis of saliva lipids in breast and prostate cancer by IR spectroscopy,” *Diagnostics*, vol. 11, no. 8, p. 1325, 2021.
- [31] N. Limsuwat, C. Boonarkart, S. Phakaratsakul, O. Suptawiwat, and P. Auewarakul, “Influence of cellular lipid content on influenza A virus replication,” *Archives of Virology*, vol. 165, no. 5, pp. 1151–1161, 2020.
- [32] I. Pérez-Torres, V. Guarner-Lans, E. Soria-Castro et al., “Alteration in the lipid profile and the desaturases activity in patients with severe pneumonia by SARS-CoV-2,” *Frontiers in Physiology*, vol. 12, Article ID 667024, 2021.
- [33] G. A. R. Ahmed, F. A. R. Khorshid, and T. A. Kumosani, “FT-IR spectroscopy as a tool for identification of apoptosis-induced structural changes in A549 cells treated with PM 701,” *International Journal of Nano and Biomaterials*, vol. 2, no. 1/2/3/4/5, pp. 396–408, 2009.
- [34] M. Pachetti, L. Zupin, I. Venturin et al., “FTIR spectroscopy to reveal lipid and protein changes induced on sperm by capacitation: bases for an improvement of sample selection in ART,” *International Journal of Molecular Sciences*, vol. 21, no. 22, p. 8659, 2020.
- [35] V. Vrbanović Mijatovic, L. Šerman, and O. Gamulin, “Analysis of pulmonary surfactant by Fourier transform infrared spectroscopy after exposure to sevoflurane and isoflurane,” *Bosnian Journal of Basic Medical Sciences*, vol. 17, no. 1, pp. 38–46, 2017.
- [36] ÓM. Peiró, A. Carrasquer, R. Sánchez-Gimenez et al., “Biomarkers and short-term prognosis in COVID-19,” *Biomarkers*, vol. 26, no. 2, pp. 119–126, 2021.
- [37] P. Malik, U. Patel, D. Mehta et al., “Biomarkers and outcomes of COVID-19 hospitalisations: systematic review and meta-analysis,” *BMJ Evidence-Based Medicine*, vol. 26, no. 3, pp. 107–108, 2021.
- [38] L. Szarpak, K. Ruetzler, K. Safiejko et al., “Lactate dehydrogenase level as a COVID-19 severity marker,” *The American Journal of Emergency Medicine*, vol. 45, pp. 638–639, 2021.
- [39] F. K. M. Chan, K. Moriwaki, and M. J. De Rosa, “Detection of necrosis by release of lactate dehydrogenase activity,” *Methods in Molecular Biology*, vol. 979, pp. 65–70, 2013.
- [40] N. Shafraan, A. Issachar, T. Shochat, I. H. Shafraan, M. Bursztyn, and A. Shlomei, “Abnormal liver tests in patients with SARS-CoV-2 or influenza - prognostic similarities and temporal disparities,” *JHEP Reports*, vol. 3, Article ID 100258, 2021.
- [41] T. L. Lin, R. D. R. Evans, R. J. Unwin, J. T. Norman, and P. R. Rich, “Assessment of measurement of salivary urea by ATR-FTIR spectroscopy to screen for CKD,” *Kidney*, vol. 3, no. 2, pp. 357–363, 2022.
- [42] Y. Wang, L. Zhang, L. Sang et al., “Kinetics of viral load and antibody response in relation to COVID-19 severity,” *Journal of Clinical Investigation*, vol. 130, no. 10, pp. 5235–5244, 2020.
- [43] S. B. Polak, I. C. Van Gool, D. Cohen, J. H. von der Thüsen, and J. van Paassen, “A systematic review of pathological findings in COVID-19: a pathophysiological timeline and possible mechanisms of disease progression,” *Modern Pathology*, vol. 33, no. 11, pp. 2128–2138, 2020.
- [44] A. Paolini, R. Borella, S. De Biasi et al., “Cell death in coronavirus infections: uncovering its role during COVID-19,” *Cells*, vol. 10, no. 7, p. 1585, 2021.
- [45] M. Eskandarian Boroujeni, A. Sekrecka, A. Antonczyk et al., “Dysregulated interferon response and immune hyperactivation in severe COVID-19: targeting STATs as a novel therapeutic strategy,” *Frontiers in Immunology*, vol. 13, Article ID 888897, 2022.
- [46] Y. M. Kim and E. C. Shin, “Type I and III interferon responses in SARS-CoV-2 infection,” *Experimental and Molecular Medicine*, vol. 53, no. 5, pp. 750–760, 2021.
- [47] M. D. Galbraith, K. T. Kinning, K. D. Sullivan et al., “Specialized interferon action in COVID-19,” *Proceedings of the National Academy of Sciences of the United States of America*, vol. 119, no. 11, Article ID e2116730119, 2022.